

Changes in temperature-precipitation correlations over Europe: Are climate models reliable?

Mathieu Vrac (✉ mathieu.vrac@lsce.ipsl.fr)

LSCE ESTIMR: Laboratoire des Sciences du Climat et de l'Environnement Equipe Extremes Statistiques Impacts et Regionalisation <https://orcid.org/0000-0002-6176-0439>

Soulivanh Thao

LSCE ESTIMR: Laboratoire des Sciences du Climat et de l'Environnement Equipe Extremes Statistiques Impacts et Regionalisation

Pascal Yiou

LSCE ESTIMR: Laboratoire des Sciences du Climat et de l'Environnement Equipe Extremes Statistiques Impacts et Regionalisation

Research Article

Keywords: Inter-variable correlations, Climate change, Statistics, Ensembles, Climate models, Reanalysis, large-scale circulation regimes

Posted Date: October 27th, 2021

DOI: <https://doi.org/10.21203/rs.3.rs-1008080/v1>

License: © ⓘ This work is licensed under a Creative Commons Attribution 4.0 International License.

[Read Full License](#)

1 Changes in temperature-precipitation
2 correlations over Europe: Are climate models
3 reliable?

4 Mathieu Vrac^{*}, Soulivanh Thao and Pascal Yiou

5 Laboratoire des Sciences du Climat et de l'Environnement
6 (LSCE-IPSL), CEA/CNRS/UVSQ, Université Paris-Saclay,
7 Centre d'Etudes de Saclay, Orme des Merisiers, 91191,
8 Gif-sur-Yvette, France.

9 ^{*}Corresponding author(s). E-mail(s): mathieu.vrac@lsce.ipsl.fr;
10 Contributing authors: soulivanh.thao@lsce.ipsl.fr;
11 pascal.yiou@lsce.ipsl.fr;

12 **Abstract**

13 Inter-variable correlations (e.g., between daily temperature and precip-
14 itation) are key statistical properties to characterise probabilities of
15 simultaneous climate events and compound events. Their correct simu-
16 lations from climate models, both in values and in changes over time,
17 is then a prerequisite to investigate their future changes and associated
18 impacts. Therefore, this study first evaluates the capabilities of one 11-
19 member multi-model ensemble (CMIP6) and one 40-member multi-run
20 single model ensemble (CESM) over Europe to reproduce the characteris-
21 tics of a reanalysis dataset (ERA5) in terms of temperature-precipitation
22 correlations and their historical changes. Next, the ensembles' correla-
23 tions for the end of the 21st century are compared to assess the robustness
24 of the future correlation changes. Over historical period, both CMIP6
25 and CESM ensembles have season-dependent and spatially structured
26 biases. Moreover, the inter-variable correlations from both ensembles
27 mostly appear stationary. Thus, although reanalyses display significant
28 correlation changes, none of the ensembles is able to reproduce them.
29 However, future correlations show significant changes over large spa-
30 tial patterns. Yet, those patterns are rather different for CMIP6 and
31 CESM, reflecting a large uncertainty in changes. In addition, for his-
32 torical and future projections, an analysis conditional on atmospheric
33 circulation regimes is performed. The conditional correlations given the

2 *Changes in temperature-precipitation correlations*

regimes are found to be the main contributor to the biases in correlation over the historical period, and to the past and future changes of correlation. These results highlight the importance of the large-scale circulation regimes and the need to understand their physical relationships with local-scale phenomena associated to specific inter-variable correlations.

Keywords: Inter-variable correlations, Climate change, Statistics, Ensembles, Climate models, Reanalysis, large-scale circulation regimes

1 Introduction

Over the last few years, the interest in statistical correlations between climate variables has become strong in various domains (e.g., [Sukharev et al, 2009](#); [Bhowmik et al, 2017](#); [Mengis et al, 2019](#); [Seo et al, 2019](#); [Tukimat et al, 2019](#), among many others). This interest comes from the fact that, most of the time, climate phenomena need to be characterised by multiple variables (precipitation, temperature, wind, etc.) and not only a single one, if we want to understand their processes and impacts. One typical example is given by the study of “compound events” (CEs), a growing field of research in the impact and climate science communities (e.g., [Zscheischler and Seneviratne, 2017](#); [Sadegh et al, 2018](#); [Zscheischler et al, 2020](#); [de Brito, 2021](#); [Ridder et al, 2021](#); [Singh et al, 2021](#); [Zscheischler et al, 2021](#), among many others). These climate events can be defined as resulting from a combination of events — not necessarily extreme by themselves — whose simultaneous or successive occurrences might generate major impacts. Different types of compound events have been categorised into a specific typology by [Zscheischler et al \(2020\)](#): “pre-conditioned” events (a weather- or climate-driven preconditioning intensifies the impacts); “multivariate” events (several simultaneous univariate hazards create the impact); “temporally compounding” events (successive hazards generate an impact); and “spatially compounding” events (univariate hazards in several places cause an impact). The key statistical aspect of such events is the dependence characterisation of the different univariate events that, together, form the CEs and cause the impacts.

In all these compound events, the dependence structure between the univariate variables or events (e.g., the correlation matrix) has to be known or estimated in a robust way. In studies investigating potential changes in CE properties and frequencies, it is thus necessary to have both correct dependence properties in the historical simulations and robust climate change signal regarding these multivariate statistical properties. More generally, this information is essential in any study relying on simulated climate data with dependence structures, such as environmental studies (in hydrology, agronomy, ecology, etc.) where the associated impact models and their output can strongly depend on the realism of the climate input, in terms of univariate properties as well as in terms of their dependence characteristics (e.g., [Ines and](#)

75 [Hansen, 2006](#); [Teutschbein and Seibert, 2012](#); [Laux et al, 2021](#)). However, it is
76 known that climate models (both Global or Regional ones, GCMs or RCMs)
77 can have biases with respect to observations or reanalyses, not only in terms
78 of marginal distributions (i.e., statistical properties of the variables considered
79 separately) but also in the multivariate properties (e.g., dependence, such as
80 correlations) of the simulations they provide (e.g., [Cannon, 2017](#); [Vrac, 2018](#);
81 [François et al, 2020](#)).

82 That is why, “bias correction” (BC) methods — also called “bias adjust-
83 ment” methods — have been developed over the last few decades. Any BC
84 method relies on a transformation of the “raw” climate simulations so that
85 the corrected simulations possess statistical properties (e.g., mean, variance,
86 or more generally their statistical distribution) similar to those of the reference
87 dataset (such as observations or reanalyses). The correction (i.e., transfor-
88 mation) is estimated over a historical period where both reference data and
89 simulations are available. The correction is supposed to be valid in a climate
90 change context and, then, applied to climate simulations over the projection
91 period of interest. BC methods can be univariate (i.e., working on one variable
92 at a time for one location at a time) or multivariate (i.e., working on several
93 variables and/or locations at the same time). In the univariate case, the
94 “quantile-mapping” approach is the most widely spread and applied technique,
95 via its multiple implementations and variants (e.g., [Haddad and Rosenfeld,](#)
96 [1997](#); [Déqué, 2007](#); [Kallache et al, 2011](#); [Vrac et al, 2012, 2016](#); [Volosciuk et al,](#)
97 [2017](#), among many others). Such a method has various advantages: it is easy
98 to implement, fast to run, and the generated corrections globally preserve the
99 main trends of the simulations (e.g., [Cannon et al, 2015](#); [Hempel et al, 2013](#)).
100 Moreover, it generally respects the ranks of the simulations to be corrected
101 and, thus, maintains the physical dependence structure of the climate model
102 (see e.g., [Vrac, 2018](#)). However, this latter point means that if the depen-
103 dence structure in the model simulations is biased, the corrections preserve
104 this biased dependence as well. This is obviously a major issue for compound
105 event estimates. Indeed, [Zscheischler et al \(2019\)](#) showed that univariate BC
106 methods (such as quantile mapping methods) are generally not sufficient to
107 reduce biases in multivariate hazard estimates and that multivariate BC meth-
108 ods should be favoured to account for dependence structures within compound
109 events. Hence, multivariate bias correction (MBC) methods aim to correct the
110 dependencies between the different variables of interest, in addition to their
111 marginal distributions. [François et al \(2020\)](#) have categorised MBC methods
112 into three types of approaches, depending on the way the dependence structure
113 is corrected: based on conditional dependencies (the “successive conditional”
114 approach, e.g., in [Piani and Haerter, 2012](#); [Dekens et al, 2017](#)); separately from
115 the marginals (“marginal/dependence”, e.g., in [Cannon, 2017](#); [Vrac, 2018](#);
116 [François et al, 2021](#)), or marginals and dependence together (“all-in-one”, e.g.,
117 [Robin et al, 2019](#); [Robin and Vrac, 2021](#)).

4 *Changes in temperature-precipitation correlations*

118 In any BC method (univariate or multivariate), one implicit or explicit
119 desirable feature is that the climate changes that are present in the raw simu-
120 lations from the calibration period to the projection one (e.g., change in mean
121 temperature, or in its moments, or change in rainfall occurrence probabili-
122 ties) are respected also by the corrected simulations. This is meant to preserve
123 the main physical information provided by climate models based on a com-
124 mon assumption: Even if climate simulations have some statistical biases, the
125 changes in the main properties are physically-driven by processes and con-
126 straints that are relevant and, thus, provide reliable information on climate
127 evolutions. Note that it is the same assumption made by the IPCC in its var-
128 ious reports when looking at anomalies (i.e., removing the seasonal cycle of
129 each climate model, which is a very simple univariate BC method) to focus
130 only on the changes (in temperature, precipitation, etc.) of the different model
131 simulations up to the end of the 21st century. Regarding evolutions of usual uni-
132 variate variables (such as temperature or precipitation separately), although
133 uncertainties are still inevitably present, the climate change signal is more
134 and more studied and robust (e.g., [Kendon et al, 2008](#); [Matte et al, 2019](#)).
135 However, signals of changes in multivariate properties or dependencies in the
136 climate simulations have not received much interest so far. Yet, these changes
137 can have major repercussions on multivariate BC designs, on compound events
138 evolutions, or more generally on conclusions brought by impact studies. Evo-
139 lution of multivariate dependence properties is then an essential signal from
140 the climate models that must be investigated to assess its reliability.

141 Moreover, local univariate and multivariate properties of climate variables
142 are influenced by large-scale synoptic atmospheric circulations (e.g., [Yiou et al,](#)
143 [2018](#); [Jézéquel et al, 2020](#); [Faranda et al, 2020](#); [Rust et al, 2013](#)). Hence,
144 biases in modeled circulations can propagate to statistical properties of local
145 climate. For example, [Maraun et al \(2021\)](#) showed that synoptic circulation
146 regimes and their biases have significant influences on univariate temperature
147 and precipitation biases and on the capability of univariate BC methods (such
148 as quantile-mapping) to correct these biases. However, the influences of atmo-
149 spheric circulation regimes on local-scale correlations or dependencies between
150 temperature and precipitation have never been investigated so far. Assessing
151 the influence of such regimes on changes of inter-variable dependence proper-
152 ties and correlations is thus an objective of the present study, as it might have
153 important consequences for applicability of MBC methods.

154 Therefore, the goal of the present paper is to assess how climate models
155 reproduce the key inter-variable dependence between temperature and pre-
156 cipitation, as well as their changes over time. To do this, we first investigate
157 how two climate model ensembles (CMIP6 multi-model ensemble and CESM
158 multi-run ensemble) compare to reference reanalysis data in terms of his-
159 torical change (i.e., evolution) of inter-variable correlations. In addition to
160 basic comparisons, we assess various contributions to the historical changes
161 in temperature-precipitation correlations, as well as to the biases of histori-
162 cal changes in correlation. This is done first by defining synoptic circulation

163 regimes and then, conditionally on each regime, by separating the marginal
164 distributions, the rank correlations (linking the marginal distributions) and
165 the circulation regimes frequencies, which all influence the inter-variable cor-
166 relations. In a second step, the conditional contributions (given the circulation
167 regimes) to future correlation changes, up to the end of the 21st century, are
168 also explored.

169 The rest of this article is structured as follows: section 2 describes the
170 reanalysis references and climate simulations used in this study. Section 3
171 assesses whether temperature-precipitation correlations from climate model
172 simulations are consistent with those from a reanalysis dataset over a his-
173 torical time period. This is done first based on direct comparisons. Next,
174 atmospheric circulation regimes are defined and basic assessments of the capa-
175 bility of the climate models to reproduce the regimes defined on reanalysis
176 data are provided. Evaluations of the changes in inter-variable correlations are
177 made via a decomposition of correlations conditional on the large-scale circu-
178 lations regimes. Section 4 characterises future changes up to the end of the
179 21st century in the simulated correlations. Finally, conclusions and discussions
180 are provided in Section 5.

181 2 Data

182 Over the historical period, the reference data used in this study come from
183 the ERA5 daily reanalysis (Hersbach et al, 2020) over the 1979-2019 period.
184 For temperature (hereafter TAS) and precipitation (PR), the western Europe
185 domain, defined as $[10^{\circ}W, 30^{\circ}E] \times [30^{\circ}N, 70^{\circ}N]$, is extracted. We select a North
186 Atlantic basin domain ($[80^{\circ}W, 30^{\circ}E] \times [30^{\circ}N, 70^{\circ}N]$) for geopotential heights
187 at 500 hPa (hereafter z500).

188 Two ensembles of climate model simulations are considered. The first one
189 is a multi-model ensemble made of 11 Global Climate Models (GCMs) con-
190 tributing to the 6th exercise of the “Coupled Models Intercomparison Project”
191 (CMIP6, Eyring et al, 2016). This selection was dictated by the availability
192 of Z500, temperature and precipitation fields on daily time scales at the time
193 of analyses: we have only selected models whose data were fully available for
194 the whole period 1979–2100. The list of the GCMs is provided in Table 1.
195 The second ensemble contains 40 members (i.e., runs) from a single GCM,
196 the “Community Earth System Model” (CESM, Kay et al, 2015) developed at
197 NCAR/UCAR (USA). The use of these two ensembles (multi-model or multi-
198 run) will allow to distinguish inter-model variability from internal variability in
199 our investigations about change in correlations. From each of these two ensem-
200 bles, the same variables (i.e., TAS, PR, z500) have been extracted for the same
201 geographical domain as for ERA5 reanalyses, over the 1979-2014 period for the
202 historical runs and over the 2015-2100 period under the shared socioeconomic
203 pathways 585 (SSP585) scenario (Riahi et al, 2017). Hence, for each run of
204 each ensemble, we consider continuous simulations from 1979 to 2100, which
205 we separate into 1980–2019 to characterise the historical period — and that

206 will be cut in 1980–1999 and 2000–2019 for historical evaluations —, as well
 207 as into four 20-year future periods: 2021–2040, 2041–2060, 2061–2080, 2081–
 208 2100. Moreover, to ease the comparisons between the different datasets, all
 209 temperature, precipitation and Z500 fields have been regridded to a common
 210 spatial resolution of $1^\circ \times 1^\circ$.

211 **3 Historical changes in inter-variable** 212 **correlations**

213 **3.1 Evaluations of historical biases and changes in** 214 **inter-variable correlations**

As a first assessment of the capability of the various climate models to reproduce the reference inter-variable correlations, Figure 1 displays the maps of the ERA5 TAS–PR correlations (ρ^{ERA5}) over the 1980–1999 period, for both winter and summer (panels 1(a) and 1(d) respectively). This figure also shows the maps of the correlation mean biases with respect to ERA5 (i.e., mean of $\rho^{model} - \rho^{ERA5}$ for all models or runs in a given ensemble) from CMIP6 (second column, 1(b) and 1(e)) and CESM runs (third column, 1(c) and 1(f)). Yet, the central question of this study is the capability of the simulations to provide changes in TAS–PR correlations over time. Hence, for each grid-cell of the domain, the change of correlation, Δ , is calculated as the difference between the 2000–2019 correlation, $\rho_{2000-2019}$, and the 1980–1999 correlation, $\rho_{1980-1999}$, i.e.,

$$\Delta = \rho_{2000-2019} - \rho_{1980-1999}, \quad (1)$$

for each model run (Δ^{run}) or for ERA5 (Δ^{ERA5}). For each ensemble (CMIP6 or CESM), the mean change of the different runs is computed to get $\overline{\Delta}^{CMIP6}$ and $\overline{\Delta}^{CESM}$. Then, the bias in *change* of correlation is defined as

$$B_{\Delta}^{ENS} = \overline{\Delta}^{ENS} - \Delta^{ERA5}, \quad (2)$$

215 where “ENS” is either CMIP6 or CESM. The last two rows of Figure 1 show,
 216 for winter and summer, the maps of these “biases in changes” of inter-variable
 217 correlations from 1980–1999 to 2000–2019, with respect to the change observed
 218 in ERA5. The equivalent maps for spring and fall are provided as supple-
 219 mentary materials in Figure SM.1. Regarding ERA5 correlations (1(a, d)), a
 220 seasonal effect is clearly visible on the spatial patterns of the correlation. This
 221 seasonal effect is also visible in the CMIP6 (1(b, e)) or CESM (1(c, f)) biases of
 222 correlation, with positive and negative patterns distributed differently accord-
 223 ing to the season. In general, correlation biases seem more pronounced with
 224 the CESM ensemble than with the CMIP6 one. This reflects the fact that,
 225 although the CESM ensemble is composed of 40 runs, as only a single climate
 226 model is used here, the runs are consistent within the ensemble and, thus, the
 227 correlations (and their biases) are similar from one run to another. For CMIP6

228 model simulations, the variability of the correlations is larger and then reduces
229 the mean correlation biases.

230 When looking at ERA5 correlation changes (1(g, j), the changes also appear
231 season-dependent. This is thus also true for the associated CMIP6 (1(h, k))
232 and CESM (1(i, l)) biases. However, here, the intensity of the biases are not
233 stronger for one ensemble. Interestingly, the spatial structures of these biases
234 in correlation changes are rather similar for the two ensembles. They both
235 look like the “negative pictures” of the structures of change seen from ERA5,
236 potentially indicating that neither CMIP6 nor CESM capture the historical
237 changes in correlations.

238 Note that significant changes in inter-variable correlations in ERA5 can
239 be caused either by internal low-frequency variability or by climate change.
240 In ERA5, the contributions of the two factors cannot be dissociated (at least
241 easily). In the CESM ensemble, the climate change signal can be estimated
242 since averaging the results obtained from different runs reduces the effect of the
243 internal variability. However, results on CESM cannot be directly transposed
244 to ERA5 as CESM can also be biased with respect to ERA5. To consider model
245 biases, it is important to analyse the CMIP6 ensemble as it provides an idea
246 of the inter-model variability. Hence, in order to investigate more these biases
247 — and more precisely the biases in changes of correlations — it is important
248 to take advantage of the ensembles and consider the distribution of changes
249 in inter-variable correlations, rather than only the mean changes across the
250 various runs.

251 3.2 Distributions of changes in correlations over 252 historical period

We investigate the distributions of changes in correlations from the CMIP6
and CESM ensembles and evaluate if they are compatible with the historical
changes seen with the ERA5 reanalyses. Therefore we define the probability
 π_{era5} that corresponds to the probability that the change in correlations —
from one reference period ($p_1=1980-1999$) to a period of interest ($p_2=2000-2019$)
as defined in Eq. (1) — is lower than or equal to the correlation change
provided by ERA5:

$$\pi_{era5} = \Pr(\Delta^{ENS} \leq \Delta^{ERA5}) \quad (3)$$

with

$$\Delta^{ENS} = \{\Delta_i = \rho(p_2, run_i) - \rho(p_1, run_i)\}_{i=1, \dots, N} \quad (4)$$

253 where N is the number of members of the ensemble “ENS” of interest ($N = 40$
254 for CESM and $N = 14$ for CMIP6). In the following, the correlation change
255 from an ensemble is said to be “compatible” at a 90% confidence level with
256 the ERA5 correlation change if $0.05 < \pi_{era5} < 0.95$, i.e., if Δ^{ERA5} lies in
257 the 90% central part of the Δ^{ENS} distribution. If $\pi_{era5} < 0.05$, the distribu-
258 tion of changes seen from the ensemble is mostly (or completely) above the
259 ERA5 change. Conversely, if $\pi_{era5} > 0.95$, the ensemble distribution from the
260 ensemble is below the ERA5 change.

261 To visualize the results, Figure 2 shows the winter and summer maps of
 262 π_{era5} probabilities for CMIP6 and CEMS, where only π_{era5} values higher than
 263 0.95 (with upper triangles) or lower than 0.05 (lower triangles) are plotted.
 264 Where no triangles are plotted, the correlation change from the ensemble is
 265 compatible with the ERA5 change.

266 To interpret these results, it is important to know where the ERA5 change
 267 in correlation is significant. Thus, a Fisher test (with a 95% confidence level) is
 268 performed based on Fisher's z -transformation (Fisher, 1915; Hotelling, 1953)
 269 to assess if the ERA5 correlations changed from one period to another. Hence,
 270 significant changes are also plotted in colours in the maps of Figure 2, while
 271 non-significant ERA5 changes are left white. The major result conveyed by
 272 Figure 2 is that, in general, for both CMIP6 and CESM, the ensemble distri-
 273 bution of changes is not compatible with an ERA5 correlation change when
 274 the latter is significant. Indeed, for many of the coloured grid cells (i.e., with
 275 significant correlation change), a triangle is also present. For negative ERA5
 276 changes (blue), a lower triangle is visible, while for positive ERA5 changes
 277 (yellow-red), it is an upper triangle. Conversely, most of the domains where
 278 the distributions of changes are compatible with ERA5 corresponds to non-
 279 significant changes. Therefore, CMIP6 and CESM do not seem to be able to
 280 reproduce the main ERA5 changes in inter-variable correlations.

281 3.3 The role of circulation regimes in historical changes

282 One can wonder how much these disagreements (between ERA5 and models) in
 283 terms of change of correlations are influenced by the disagreements in frequen-
 284 cies between ERA5 and simulated circulations. Do the partial disagreements in
 285 changes of correlations come from the biased simulated regime frequencies? Or
 286 from biases in the marginal properties (of temperature and precipitation) con-
 287 ditionally on the regimes? From biased conditional temperature-precipitation
 288 correlations, given a regime? If they come from a combination of such features,
 289 what are their relative contributions? To answer such questions, it is necessary
 290 to define these regimes.

291 3.3.1 Circulation regimes: definition and basic GCM 292 assessment

293 For each of the four seasons separately (winter: DJF; spring: MAM; summer:
 294 JJA; fall: SON), the ERA5 daily z500 fields are pre-processed in two steps: (i)
 295 they are first deseasonalized and detrended. For that, the seasonality is esti-
 296 mated and removed by fitting a smoothing spline over the spatially averaged
 297 z500 over all years as a function of the day in the year. The temporal trend is
 298 then computed and removed as a smoothing spline of the deseasonalized Z500
 299 as a function of time; (ii) a Principal Component Analysis (PCA) is performed
 300 on the detrended and deseasonalized fields. The principal components (PC)
 301 explaining 90% of the total variance are kept (12 PCs in DJF, 14 in MAM and
 302 SON, 17 in JJA).

303 Then, for each of the four seasons separately, based on the PCs retained,
304 the k-means clustering algorithm is applied to define $K = 4$ regimes. Here, this
305 number $K = 4$ is arbitrarily selected to be consistent with circulation regimes
306 found in the literature (e.g., Michelangeli et al, 1995; Corti et al, 1999; Yiou and
307 Nogaj, 2004). The k-means algorithm is performed with the Hartigan-Wong
308 algorithm (Hartigan and Wong, 1979) with a maximal number of iterations
309 equal to 100. Since the algorithm is sensitive to the cluster initialization, the
310 algorithm is performed for 10 random cluster initialisations. The clustering for
311 which the within sum of squares is minimum is kept. The four resulting ERA5
312 composite maps for Winter are shown in Fig. 3. We obtain the four traditional
313 circulation regimes in winter: map 3(a) corresponds to the “Blocking” regime,
314 3(b) to the “Atlantic Ridge” one, 3(c) to the positive phase of the North
315 Atlantic Oscillation (NAO+) and 3(d) to its negative phase.

316 Each CMIP6 and CESM daily Z500 field is next attributed to one of the
317 ERA5 regimes. The following steps are performed:

- 318 1. The daily Z500 fields from the models are pre-processed by removing the
319 average temporal trend and seasonality over North Atlantic in the same way
320 as for ERA5. Note that the trend and seasonality is estimated individually
321 for each dataset (i.e., run).
- 322 2. Each detrended and deseasonalized daily Z500 field is projected onto the
323 selected principal components defined from the ERA5 dataset, in order to
324 get the PCs characterising this day. The projection is made thanks to the
325 PCA rotation matrix obtained with the ERA5 dataset.
- 326 3. Finally, a day is attributed to a given circulation regime if the Euclidean distance
327 between the PCs of this day and the PCs of the centroid representing
328 the regime is minimum.

329 Hence, the circulation regimes are forced to be the same for the model simu-
330 lations and for the reanalyses. By construction, the CESM and CMIP6
331 composite maps obtained for each regime are then very close to those from
332 ERA5 (not shown). Note that the CESM and CMIP6 historical simulations
333 do not represent the chronology of observations but it is assumed that each
334 model simulates its own meteorology that its consistent with the chronology
335 of natural and anthropogenic forcings. Therefore, although the chronological
336 sequences are different, it is expected that the statistics are comparable. This
337 must be reflected in the regimes and their frequencies. So, it is meaningful to
338 compare ERA5’s regimes to CMIP6/CESM’s, even if the chronologies are not
339 the same. However, a basic evaluation of the frequencies of each regime indi-
340 cates some differences between the frequencies from the ERA5 regimes and
341 those from CESM or CMIP6, as shown in Fig. 4 for the four seasons.

342 At first sight, the frequencies from models appear to be biased with respect
343 to the reference ERA5 frequencies. However, the ranges of frequencies in Fig. 4
344 are quite tight, visually emphasising the biases. Generally, the inter-model
345 variability of the frequencies from the CMIP6 models is slightly higher than
346 the inter-run variability brought by the CESM runs, in particular in summer

347 and fall. Nevertheless, most of the time, the frequency biases are somehow
348 equivalent for CMIP6 models and CESM runs: they generally both either
349 overestimate or underestimate the ERA5 frequencies, with the exception of
350 cluster 4 in winter. These biases in frequencies can be quite pronounced. In
351 many cases, the reference ERA5 frequency is out of the inter-quartile inter-
352 val (e.g., C3 in winter among others), and even out of the whole boxplot (i.e.,
353 distribution), as in regime C2 for CESM, or in regime C3 in fall for both
354 CMIP6 and CESM. Corti et al (1999) speculated that the increase in temper-
355 ature over the Northern Hemisphere may be due to a change in the frequency
356 of the regimes. This is about the same idea investigated here but in terms
357 of change of (temperature-precipitation) inter-variable correlation, instead of
358 change of temperature. Even if the conditional temperature-precipitation cor-
359 relation given this regime is correct (which is not assessed so far), the frequency
360 biases can have major consequences on the overall inter-variable correlation.

361 Hence, it is interesting to look at the conditional biases of the inter-variable
362 (temperature vs. precipitation) correlations given the weather regimes, as well
363 as the conditional biases of changes in inter-variable correlations, given the
364 weather regimes. Those are given for the four seasons in Figures SM.6–SM.9
365 and SM.10–SM.13 of the supplementary materials section but are mostly
366 described for winter below. Regarding ERA5 correlation maps (first columns of
367 Figures SM.6–SM.9), roughly speaking, the spatial structure of the correlations
368 is rather similar for unconditional or conditional calculations, with, in winter, a
369 latitudinal gradient, going from strong positive correlation values towards the
370 North, e.g., along the Norwegian coast, to strong negative correlations towards
371 the South, e.g., over the Mediterranean region. However, the magnitude of
372 these correlations varies from one circulation regime to another, reflecting their
373 influences. For example, winter regime 2 (panel SM.6(g)) induces the strongest
374 TAS-PR correlations over Finland and mild ones over France, while regime 3
375 (panel SM.6(j)) displays mild correlations over Finland and the weakest cor-
376 relations over France. The spatial structures of the CMIP6 maps of winter
377 mean biases are also quite similar for unconditional and conditional calcula-
378 tions whatever the regime: A central band going from Spain and France to
379 the East (to Poland and Belarus) shows correlation biases close to zero or
380 slightly negative, while out of this band (i.e., to the North or South), most of
381 the biases are positive. Nevertheless, as for ERA5 correlation maps, the biases
382 show some variability. For example, winter regime 2 (panel SM.6(h)) is the
383 only circulation type presenting almost no bias (or slightly negative) over Fin-
384 land, and quite strongly positive biases over Greece. The spatial structure of
385 the CESM TAS-PR correlation mean biases (third column) is quite different
386 and more pronounced than that of CMIP6 average. As for CMIP6, although
387 some variability is visible, the winter CESM pattern of biases is relatively
388 the same from one regime to another. However, the magnitude of the mean biases
389 is much stronger, inversely following the ERA5 correlations: highly negative
390 biases (i.e., underestimating the correlations) to the North and highly positive
391 biases (i.e., overestimating the correlations) to the South.

392 Regarding ERA5 conditional changes of correlations (Figures SM.10–
 393 SM.13, panels (a, d, g, j, m)), here, the weather regimes conditioning brings
 394 signals different from the unconditional changes of correlations, with a high
 395 variability of change from one regime to another. More pronounced changes —
 396 both increasing or decreasing — are visible with spatial structures appearing
 397 when looking at changes conditional on the circulation regimes, for example,
 398 for winter regimes 2 and 4 (panels SM.10(g, m)), or for fall regime 4 (panels
 399 SM.13(m)). Regarding CMIP6 or CESM conditional biases in changes of cor-
 400 relation, they are somehow equivalent to each other. Interestingly, as already
 401 observed for the unconditional case, they mostly correspond to the “negative
 402 pictures” of the ERA5 maps of changes, indicating that CMIP6 and CESM
 403 ensembles do not see much of the historical changes and tend to have stationary
 404 TAS-PR correlations from 1980-1999 to 2000-2019, both in the unconditional
 405 and conditional cases.

406 3.3.2 Conditional decomposition of correlation

In order to investigate some role of the defined circulation regimes in the
 (historical or future) changes of inter-variable correlations, we rely on a decom-
 position of the correlation that is applicable when the statistical population
 (our daily time series) is composed of clusters (here, circulation regimes). This
 decomposition of correlation was introduced by Charter and Alexander (1993).
 Based on a bivariate time series $(x_i, y_i)_{i=1, \dots, N}$ (here, temperature and pre-
 cipitation at a given gridcell) that is clustered in K groups (here, $K = 4$
 circulation regimes) of size $(n_k)_{k=1, \dots, K}$, the correlation between X and Y can
 be decomposed into:

$$\rho = \frac{N\Sigma XY - (\Sigma X)(\Sigma Y)}{\sqrt{N\Sigma X^2 - (\Sigma X)^2} \sqrt{N\Sigma Y^2 - (\Sigma Y)^2}} \quad (5)$$

407 where

- 408 • $N = \sum_{k=1}^K n_k$ is the total sample size,
- 409
- 410 • $\Sigma X = \sum_{k=1}^K (n_k \bar{X}_k)$ and $\Sigma Y = \sum_{k=1}^K (n_k \bar{Y}_k)$,
- 411
- 412 • $\Sigma X^2 = \sum_{k=1}^K n_k (\bar{X}_k^2 + S_{X_k}^2)$ and $\Sigma Y^2 = \sum_{k=1}^K n_k (\bar{Y}_k^2 + S_{Y_k}^2)$,
- 413
- 414 • $\Sigma XY = \sum_{k=1}^K n_k (\rho_k S_{X_k} S_{Y_k} + \bar{X}_k \bar{Y}_k)$,

415 where ρ_k is the k^{th} subgroup correlation between X and Y , S_{X_k} and S_{Y_k} are the
 416 k^{th} subgroup standard deviations, and \bar{X}_k and \bar{Y}_k are the k^{th} subgroup sample
 417 means. Thus, based on equation (5), it is possible to calculate the uncondi-
 418 tional correlation between X and Y if we know $\mathbf{n} = \{n_k\}_{k=1, \dots, K}$ (i.e., sizes
 419 of the K clusters), $\mathbf{M} = \{\bar{X}_k, \bar{Y}_k, S_{X_k}, S_{Y_k}\}_{k=1, \dots, K}$ (i.e., the marginal
 420 properties of each cluster) and $\mathbf{P} = \{\rho_k\}_{k=1, \dots, K}$ (i.e., the X vs. Y correlation

in the K clusters). Hence, if the three types of information — cluster sizes, conditional marginal properties and conditional correlations, hereafter referred to as “weather regimes conditional information” $\mathbf{WRCI} = (\mathbf{WRCI}_k)_{k=1,\dots,K} = (\mathbf{n}, \mathbf{M}, \mathbf{P}) = (n_k, M_k, \rho_k)_{k=1,\dots,K}$ — are calculated for one climate model simulation (\mathbf{WRCI}^{mod}) and for the ERA5 references (\mathbf{WRCI}^{ref}), we can compute (i) the influence of the bias of each given \mathbf{WRCI} component on the bias in change of correlation, as well as (ii) the contribution of the change of each given \mathbf{WRCI} component to the change of the correlation over time.

3.3.3 Influences of the “Weather Regimes Conditional Information” biases on the biases of historical changes in correlations

We define the change in correlation as $\Delta = \rho_2 - \rho_1$, where subscripts “1” and “2” refer respectively to a past (e.g., 1980–1999) period and to a more recent (e.g., 2000–2019) period. For a given period p (either p_1 or p_2), the ERA5 correlation ρ between X (temperature) and Y (precipitation) can be calculated using Eq. (5), knowing the three \mathbf{WRCI} components ($\mathbf{n}, \mathbf{M}, \mathbf{P}$) estimated from the ERA5 dataset. The ERA5 correlation can then be noted as $\rho^{WRCI_{ERA5,p}}$ where $WRCI_{ERA5,p} = (\mathbf{n}^{(ERA5,p)}, \mathbf{M}^{(ERA5,p)}, \mathbf{P}^{(ERA5,p)})$ corresponds to the ERA5 \mathbf{WRCI} components calculated over period p . Likewise, the correlation from a run in the CMIP6 or CESM ensemble over period p can be written as $\rho^{WRCI_{run,p}}$ with $WRCI_{run,p} = (\mathbf{n}^{(run,p)}, \mathbf{M}^{(run,p)}, \mathbf{P}^{(run,p)})$ corresponding to the run \mathbf{WRCI} s. For this run, the change in correlation from period p_1 to period p_2 is then $\Delta^{run} = \rho^{WRCI_{run,p_2}} - \rho^{WRCI_{run,p_1}}$. For ERA5, it is $\Delta^{ERA5} = \rho^{WRCI_{ERA5,p_2}} - \rho^{WRCI_{ERA5,p_1}}$. The bias in the change of correlation for this run is then $\Delta^{run} - \Delta^{ERA5}$. However, it is possible to calculate the change that would have occurred for this run if one of the \mathbf{WRCI} components over the two periods was correct, i.e., was the same as that of the ERA5 reference. For example, in the case of a correct \mathbf{n} components, this hypothetical change of correlation, denoted as $\Delta^{WRCI|\mathbf{n}}$, is calculated as the change that is obtained when computing the correlations (over p_1 and p_2 periods) with an \mathbf{n} component from the reference ERA5 data, while the other \mathbf{WRCI} components \mathbf{M} and \mathbf{P} stem from the run itself:

$$\Delta^{WRCI|\mathbf{n}} = \rho^{(\mathbf{n}^{(ERA5,p_2)}, \mathbf{M}^{(run,p_2)}, \mathbf{P}^{(run,p_2)})} - \rho^{(\mathbf{n}^{(ERA5,p_1)}, \mathbf{M}^{(run,p_1)}, \mathbf{P}^{(run,p_1)})}. \quad (6)$$

The bias of this correlation change is then $\Delta^{WRCI|\mathbf{n}} - \Delta^{ERA5}$. Hence, for this specific run, the influence of the bias of a given \mathbf{WRCI} component (here, \mathbf{n} for the example) on the bias in change of correlation is noted as $Ib(\mathbf{n})$ and is defined as:

$$Ib(\mathbf{n}) = \frac{|\Delta^{run} - \Delta^{ERA5}| - |\Delta^{WRCI|\mathbf{n}} - \Delta^{ERA5}|}{|\Delta^{run} - \Delta^{ERA5}|} = 1 - \frac{|\Delta^{WRCI|\mathbf{n}} - \Delta^{ERA5}|}{|\Delta^{run} - \Delta^{ERA5}|} \quad (7)$$

and corresponds to the reduction of bias in terms of change of correlation that is brought by having ‘a ‘correct’ \mathbf{n} **WRCI** information. The influences $Ib(\mathbf{M})$ and $Ib(\mathbf{P})$ of the **WRCI** components other than \mathbf{n} can be calculated the same way by permuting ‘ERA5’ and ‘run’ labels at the appropriate locations in Eq. (6) to compute $\Delta^{WRCI|\mathbf{M}}$ and $\Delta^{WRCI|\mathbf{P}}$, allowing to get $Ib(\mathbf{M})$ and $Ib(\mathbf{P})$ from Eq. (7).

For each of the three **WRCI** components, in order to get a single Ib value for each ensemble and gridcell, the N Ib values given for a given gridcell by the different runs or models in an ensemble (CMIP6 or CESM) are averaged. Fig. 5 displays the boxplots of the influences of the three **WRCI** components to the CMIP6 (red) and CESM (green) biases of changes in winter temperature-precipitation correlations from 1980-1999 to 2000-2019 for the four seasons.

Generally speaking, all seasons give qualitatively similar results, which are also very similar for CMIP6 and CESM ensembles: the major influence on the biases in change in correlations come from the biases in the \mathbf{P} component, explaining on average about 75% of the biases in correlation change. The biases in \mathbf{M} , conditional marginal distributions, mostly explain the remaining 25%, while the biases in \mathbf{n} , the size (i.e., frequency) of the circulation regimes, does not influence the biases in correlation changes. Some differences appear however when looking more closely at the results. For example, while the influence of the conditional correlations is very strong for spring (5.b) and summer (5.c), pushing down the relative influence of the conditional marginal distributions, the winter and overall fall seasons (Fig. 5a and Fig. 5d) see more pronounced influences of the conditional distributions, thus reducing the influence of the conditional correlations.

The main conclusion is that, although the conditional marginal properties have some moderate influences, the biases in conditional correlations — given the circulation regimes — are the main drivers of the biases in correlation changes over the historical period. The regime frequency biases being relatively small (Fig. 4, their influence appears almost negligible).

3.3.4 Contributions of the ‘Weather Regimes Conditional Information’ changes to the historical changes of correlations

In addition, whether they are biased or not, the Conditional Information can change over time and it is important to know how much these conditional changes contribute to the change of the unconditional TAS-PR correlation. To quantify the contribution of the change of a given **WRCI** component — say \mathbf{n} for the illustration — to the change in inter-variable correlation, the correlations over the two period p_1 and p_2 are calculated based on Eq. (5) by considering that the **WRCI** component of interest (e.g., \mathbf{n}) is stationary over time, i.e., is the same for the two periods. Hence, for the \mathbf{n} example,

$$\rho^{data,p_1} = \rho^{\mathbf{WRCI}_{data,p_1}} = \rho^{(\mathbf{n}^{(data,p_1)}, \mathbf{M}^{(data,p_1)}, \mathbf{P}^{(data,p_1)})}$$

and

$$\rho^{data,p2|\mathbf{n}} = \rho^{(\mathbf{n}^{(data,p1)}, \mathbf{M}^{(data,p2)}, \mathbf{P}^{(data,p2)})} \quad (8)$$

where “data” is either “ERA5” or the “run” of a model. The important point to note is that, here, $\rho^{data,p2|\mathbf{n}}$ is calculated with a stationary **WRCI** \mathbf{n} component estimated from period 1: hence, the \mathbf{n} components are the same for the two periods. The hypothetical change between these two correlations is

$$\Delta^{data|\mathbf{n}} = \rho^{data,p2|\mathbf{n}} - \rho^{data,p1}.$$

The contribution of the change in the \mathbf{n} component to the change of the unconditional correlation is then quantified as:

$$C_{\Delta}(\mathbf{n}) = \frac{\Delta^{data} - \Delta^{data|\mathbf{n}}}{\Delta^{data}} = 1 - \frac{\Delta^{data|\mathbf{n}}}{\Delta^{data}}. \quad (9)$$

465 The contributions $C_{\Delta}(\mathbf{M})$ and $C_{\Delta}(\mathbf{P})$ of the conditional information other
 466 than \mathbf{n} can be calculated the same way by permuting “ p_1 ” and “ p_2 ” labels
 467 at the appropriate locations in Eq. (8) to compute $\rho^{data,p2|\mathbf{M}}$ and $\rho^{data,p2|\mathbf{P}}$,
 468 allowing to get $C_{\Delta}(\mathbf{M})$ and $C_{\Delta}(\mathbf{P})$ from Eq. (9).

469 As previously, for each of the three **WRCI** components, in order to get
 470 a single C_{Δ} value for each ensemble and gridcell, the N C_{Δ} values given for
 471 a given gridcell by the different runs or models in an ensemble (CMIP6 or
 472 CESM) are averaged. Figure 6 shows the boxplots of contribution values of
 473 the changes in the three **WRCI** components to the changes in temperature-
 474 precipitation correlations from 1980-1999 to 2000-2019 for the four seasons, for
 475 CMIP6 and CESM ensembles as well as for ERA5. As for Figure 5, a relatively
 476 similar behaviour can be observed for the four seasons as well as for the differ-
 477 ent datasets: the major part of the unconditional correlation changes is due to
 478 the changes in the conditional correlations given the circulation regimes. The
 479 changes in conditional marginal properties only contribute at a quite moderate
 480 level, while the contribution values of the changes in frequencies of the regimes
 481 are centered around 0. The ensembles (CMIP6 and CESM) **WRCI** contribu-
 482 tions are consistent with those from ERA5. However, for winter and fall
 483 (panels 6.a and 6.d), the contributions of the **WRCI** components are somehow
 484 different between ERA5 and the two ensembles: the CMIP6 and CESM contribu-
 485 tions are stronger for the \mathbf{P} components, while their \mathbf{M} contributions are
 486 underestimated. Interestingly, this coincides with a similar pattern observed in
 487 Fig. 5 for **WRCI** influences on biases of changes. This means that, for winter
 488 and fall, the changes in unconditional correlation are biased not only by the
 489 values of the conditional correlations but also by the changes in the conditional
 490 correlation values, i.e., the time evolutions of the conditional correlations. For
 491 spring and summer, the agreement in terms of relative contributions between
 492 the three datasets suggests that the time evolution of the conditional correla-
 493 tions is not the main contributor of the biases in changes of correlations, and
 494 that — as shown in Fig. 5 — the biases of the conditional correlation values
 495 themselves correspond to the major reasons.

4 Projections of future changes in inter-variable correlations

A natural question is then whether, in a future climate, the changes in inter-variable TAS-PR correlations will continue to be mostly driven by changes in conditional correlations or if changes in frequencies of the circulation regimes or in conditional marginal properties will take over. To do so, the CMIP6 and CESM simulations up to 2100 are used, with a focus on the 2081-2100 period. In this context, the goal is not to perform an evaluation of of the simulated changes — as no reference is available for comparison in the future — but to characterise if CMIP6 and CESM ensembles provide significant changes in inter-variable correlations in the future simulations, and if so, how these changes are driven by the conditional changes, given the circulation structures.

4.1 Distributions of changes in correlations in future projections

First, for each given ensemble, season and grid cell, the mean correlation over 1981-2000 is compared to the mean correlation over 2081-2100 based on a Student t test at a 95% significant level. Values of change in mean correlations (i.e., mean 2081-2100 correlation minus mean 1981-2000 correlation) found significant are plotted in Figure 7 for CMIP6 and CESM, and winter and summer. In addition, similarly to Eq. (3) that defines π_{era5} , the probability that the changes from an ensemble is lower than the ERA5 correlation change, π_0 is now computed as the probability that the changes from an ensemble is lower than 0.

$$\pi_0 = \Pr(\Delta^{ENS} \leq 0) \quad (10)$$

where Δ^{ENS} is defined as in Eq. (4). Thus, the probability π_0 indicates where the “no change” case is located in the ensemble distribution of changes in correlations from 1981-2000 to 2081-2100. This information is superimposed into Figure 7, only for $\pi_0 < 0.05$ (as lower triangles) indicating that a zero change is in the lower tail of the distribution, and for $\pi_0 > 0.95$ (as upper triangles) indicating that a zero change is in the upper tail. These two cases can thus be interpreted as opposite but significant changes of correlations. Hence, where no triangle is plotted, a stationary correlation between the two time periods cannot be rejected. Contrary to the results over the historical period (Fig. 2) that showed that, in general, CMIP6 and CESM are not able to reproduce the main ERA5 significant changes in inter-variable correlations, here, the correlation changes up to 2081-2100 indicate that the “no change” case is regularly excluded (upper and lower triangles in Fig. 7). Moreover, this rejection is made for a very large portion of the patterns identified with a significant change in mean correlation, implying that the changes in correlation distributions are sufficiently strong to significantly reject the “no change” case. Nevertheless, it is also clear here that CMIP6 and CESM ensembles do not show a strong agreement on this change of correlation criterion: for example, patterns of significant change in mean correlations — as well π_0 triangles —

529 are very distinct in summer for CMIP6 (7.b) and CESM (7.d). Hence, although
530 significant changes of correlations are simulated by the models, their variability
531 between models (as in CMIP6) or between ensembles (CMIP6, CESM) is quite
532 strong, questioning the robustness of these changes.

533 4.2 Contributions of the circulation regimes to the 534 future changes of correlations

535 In order to know how these changes in inter-variable correlations and their
536 disagreements between CMIP6 and CESM are driven by the conditional infor-
537 mation brought by the circulation regimes, Figure 8 displays the boxplots
538 of contribution values of the change in the three **WRCI** components to the
539 changes in temperature-precipitation correlations from 1981-2000 to 2081-2100
540 for the four seasons and for CMIP6 and CESM ensembles. These contributions
541 are calculated following Equation (9) for each grid point showing a significant
542 change between the two periods. Like in Fig. 6 over the historical period, the
543 contribution of the regime frequencies (component **n**) to future unconditional
544 correlation changes is close to zero, although slightly bigger and with a slightly
545 higher variability. However, contributions of future conditional marginal prop-
546 erties (component **M**) are smaller than for the historical period and are now
547 relatively equivalent to those from regime frequencies. This implies that the
548 vast majority of the contributions comes from the changes in conditional cor-
549 relations (component **P**) given the circulation regimes, although some differences
550 between CMIP6 and CESM are visible. If this was already true over the his-
551 torical period, it is reinforced within the future projections for both CMIP6
552 and CESM ensembles.

5 Conclusions and discussion

This study investigated first the capability of two climate model ensembles — one multi-model (CMIP6) and one multi-run from a single model (CESM) — to reproduce the historical inter-variable temperature vs. precipitation correlations from ERA5 reanalyses over Europe, as well as their changes over the historical period 1980-2019. As ERA5 inter-variable correlations are season dependent, so are the associated model biases, with distinct patterns for CMIP6 and CESM (Fig. 1.a-f). Some changes in ERA5 TAS vs. PR correlations from 1980-1999 to 2000-2019 were found significant, also with spatial structures depending on seasons. However, both CMIP6 and CESM biases of changes are almost the exact “negative picture” of the ERA5 changes (Fig. 1.g-l), indicating that these ensembles do not show changes of the inter-variable correlations over the 1980-2019 period. This has been further analysed by a comparison between the ERA5 correlation changes and the ensembles distributions of correlation changes (Fig. 2), showing that, most of the ERA5 significant changes belong to the lower (i.e., $< 5^{th}$ percentile) or upper tail (i.e., $> 95^{th}$ percentile) of the distribution, therefore out of the 90% confidence interval of the simulated changes. These results confirmed the inability of the tested ensembles to reproduce the ERA5 historical changes in correlations.

Second, to try understanding if/how these mismatches between ERA5 and ensembles are driven by some large-scale atmospheric circulation structures, conditional analyses have been performed. First, circulation regimes (or clusters) have been defined for each season separately (Fig. 3), via a k-means algorithm applied to daily fields of geopotential heights at 500 hPa (Z500). Then, simulated Z500 fields from 1980 to 2100 have been classified into the regimes. Although the ensembles regimes frequencies were shown to have more or less errors depending on the seasons (Fig. 4), this may not be the only reason of the mismatches. Other regimes-related statistical properties can also contribute, such as the conditional TAS vs. PR correlations or the conditional marginal properties of TAS and PR, both given the regimes. Hence, based on a mathematical decomposition of the correlation (Eq. (5)), the influences of the biases of the size of the regimes (\mathbf{n}), the conditional correlations (\mathbf{P}) and the conditional marginal properties (\mathbf{M}), both given fixed clusters, onto the mismatches have been investigated. The results (Fig. 5) showed that the bias of the size of the regimes have a rather negligible effect on the (unconditional) correlation biases, while the misrepresentation of the marginal TAS and PR properties (means and variances) has a stronger influence ($\sim 25\%$) on the final correlation bias. However, the major influence is due to the conditional correlation, whose the biases explains about 75% of the unconditional correlation. Moreover, the contribution of the changes (from 1980-1999 to 2000-2019) in the three conditional properties (\mathbf{n} , \mathbf{M} , \mathbf{P}) to the changes in the unconditional correlations is distributed the same way (Fig. 6): quite small for \mathbf{n} , $\sim 20\%$ for \mathbf{M} and $\sim 80\%$ for \mathbf{P} . In addition, a comparison to ERA5 over the historical period (Fig. 6) shows that, although the ensembles conditional contributions

598 have equivalent structures as ERA5's, the contributions of the conditional
599 correlation are generally overestimated by the models (essentially for winter,
600 summer and fall), at the expense of the contributions from the conditional
601 marginals properties that are, thus, rather underestimated.

602 Hence, the general answer to the question “Are climate models reliable
603 in terms of changes in temperature-precipitation correlations?”, asked in the
604 title, is “no”. Clear biases with respect to ERA5 are present in terms of TAS
605 vs. PR correlations, as well as in terms of changes (over 1980-2019) of these
606 correlations, with inappropriate contributions of changes from the WRCI
607 components.

608
609 Next, future changes in correlations have also been investigated for the
610 two ensembles, based on 2081-2100 TAS vs. PR correlations with respect to
611 those from 1981-2000. Significant changes were found (Fig. 7) with season
612 dependent patterns but quite different for CMIP6 and CESM. This reflects a
613 not-so-robust signal in terms of future evolution of the correlations. The anal-
614 ysis of the different “weather regimes conditional information” components
615 (\mathbf{n} , \mathbf{M} , \mathbf{P}) showed that the future changes in conditional correlations provide
616 the largest contributions to the future changes in unconditional correlations
617 (\mathbf{P}), for both ensembles (Fig. 8). This was already true over the historical
618 period and will continue — and will even be slightly reinforced — in future
619 SSP585 climate scenario.

620
621 These results highlight the importance of the large-scale circulation struc-
622 tures/regimes and the need to understand their physical relationships with
623 local-scale phenomena associated to specific inter-variable correlations. If these
624 relationships are misrepresented within climate models, the local-scale cor-
625 relations related to circulations (i.e., conditional correlations), as well as their
626 changes in time, can be biased. This can lead to major biases in the uncon-
627 ditional inter-variable correlations and therefore on the simulated compound
628 events. Hence, various perspectives and future works can be envisioned from
629 this study.

630 First, TAS and PR are obviously not the only climate variables. Equivalent
631 studies could be performed for variables other than TAS and PR, for example,
632 analysing correlations between wind and PR, or humidity and TAS, etc. Also,
633 inter-variable correlations are not the only dependence property of interest in
634 the climate system. Equivalent studies for spatial dependencies and/or tempo-
635 ral dependencies (e.g., auto-correlations and/or cross-auto-correlations) could
636 be carried out.

637 Moreover, more generally, our results strongly motivate not only to improve
638 climate models in terms of relationships between spatial scales but also
639 to continue developing and improving multivariate bias correction (MBC)
640 methods, allowing to make (e.g., inter-variable) dependencies more realistic.
641 However, as this study showed that large-scale structures have influences on
642 the local/regional-scale dependencies and, thus, on their biases, MBC must

643 include large-scale information into the correction process. One “easy” pos-
644 sibility for this is to condition MBC applications on circulation regimes but
645 other ways could be defined. This would allow MBC methods to be physically
646 driven.

647 Nevertheless, signals in terms of future evolution of TAS vs. PR correla-
648 tions were found to be present but not very robust, i.e., with a large variability
649 within the CMIP6 ensemble, and overall a large variability between the CMIP6
650 and CESM ensembles. This asks the question of whether and how simulated
651 future changes in inter-variable correlations should be accounted for. If the sim-
652 ulated changes of correlation are meaningless or considered not robust enough,
653 the many compound events (CE) analyses in a future climate context should
654 rather rely on a stationarity assumption for the dependence structures, only
655 allowing to change the marginal distributions and properties of the variables of
656 interest. This could be made by estimating the dependence properties from a
657 reference dataset over a historical period and, then, injecting them into future
658 climate simulations instead of their dependence. Obviously, this could have
659 major consequences on the CE results and must be investigated with caution.

660 This question of stationarity assumption of the dependence structure
661 also matters for multivariate bias correction design. Indeed, if changes in
662 multivariate dependence (e.g., correlation) in the climate simulations are
663 reliable, MBCs have to reproduce them and generate corrections with similar
664 changes. However, if these simulated changes are not robust, MBC could rely
665 on a stationarity assumption of the dependence from the reference dataset.
666 Hence, the multivariate properties (e.g., correlations) would not evolve and
667 stay similar to the reference. Understanding the robustness of the changes in
668 simulated dependencies is thus key to choose and apply the appropriate MBC
669 methods in climate change context.

670

671 **Supplementary information**

672 This article has supplementary materials.

673 **Acknowledgments**

674 We acknowledge the World Climate Research Programme’s Working Group on
675 Coupled Modelling, which is responsible for CMIP, and we thank the climate
676 modeling groups (listed in Table 1 of this paper) for producing and making
677 available their models outputs. For CMIP, the U.S. Department of Energy’s
678 Program for Climate Model Diagnosis and Intercomparison provides coordi-
679 nating support and led development of software infrastructure in partnership
680 with the Global Organization for Earth System Science Portals. We also thank
681 the Copernicus Climate Change Services for making the ERA5 reanalyses
682 available.

Funding

MV has been supported by the CoCliServ project, which is part of ERA4CS, an ERA-NET initiated by JPI Climate and cofunded by the European Union (grant no. 690462). MV has also been supported by project C3S 428J (“HR-CDFt”).

Competing interests

The authors declare that no competing interests are present.

Availability of data and materials

The CMIP6 model simulations can be downloaded through the Earth System Grid Federation portals. Instructions to access the data are available here: <https://pcmdi.llnl.gov/mips/cmip5/data-access-getting-started.html>. The ERA5 reanalysis data used as reference in this study can be accessed via the “Climate Data Store” (CDS) web portal <https://cds.climate.copernicus.eu>.

Authors’ contributions

MV had the initial idea of the study, developed the associated codes for the analyses and made the figures. All authors contributed to the methodology and the analyses. MV wrote the article with inputs from ST and PY.

References

- Bhowmik RD, Sankarasubramanian A, Sinha T, et al (2017) Multivariate downscaling approach preserving cross correlations across climate variables for projecting hydrologic fluxes. *Journal of Hydrometeorology* 18(8):2187 – 2205. <https://doi.org/10.1175/JHM-D-16-0160.1>, URL <https://journals.ametsoc.org/view/journals/hydr/18/8/jhm-d-16-0160.1.xml>
- Boucher O, Denvil S, Levvasseur G, et al (2018) IPSL IPSL-CM6A-LR model output prepared for CMIP6 CMIP. <https://doi.org/10.22033/ESGF/CMIP6.1534>, URL <https://doi.org/10.22033/ESGF/CMIP6.1534>
- Cannon A (2017) Multivariate quantile mapping bias correction: An n-dimensional probability density function transform for climate model simulations of multiple variables. *Clim Dyn* <https://doi.org/10.1007/s00382-017-3580-6>
- Cannon AJ, Sobie SR, Murdock TQ (2015) Bias correction of gcm precipitation by quantile mapping: How well do methods preserve changes in quantiles and extremes? *Journal of Climate* 28(17):6938 – 6959. <https://doi.org/10.1175/JCLI-D-14-00703.1>

- 716 [//doi.org/10.1175/JCLI-D-14-00754.1](https://doi.org/10.1175/JCLI-D-14-00754.1), URL [https://journals.ametsoc.org/
717 view/journals/clim/28/17/jcli-d-14-00754.1.xml](https://journals.ametsoc.org/view/journals/clim/28/17/jcli-d-14-00754.1.xml)
- 718 Charter R, Alexander R (1993) A note on combining correlations. *Bull Psy-*
719 *chon Soc* 31:123–124. <https://doi.org/10.3758/BF03334158>, URL [https://
720 doi.org/10.3758/BF03334158](https://doi.org/10.3758/BF03334158)
- 721 Corti S, Molteni F, Palmer T (1999) Signature of recent climate change in
722 frequencies of natural atmospheric circulation regimes. *Nature* 398:799–802.
723 <https://doi.org/10.1038/19745>
- 724 de Brito MM (2021) Compound and cascading drought impacts do not
725 happen by chance: A proposal to quantify their relationships. *Sci-*
726 *ence of The Total Environment* 778:146,236. [https://doi.org/https://doi.
727 org/10.1016/j.scitotenv.2021.146236](https://doi.org/https://doi.org/10.1016/j.scitotenv.2021.146236), URL [https://www.sciencedirect.com/
728 science/article/pii/S0048969721013048](https://www.sciencedirect.com/science/article/pii/S0048969721013048)
- 729 Dekens L, Parey S, Grandjacques M, et al (2017) Multivariate distribution
730 correction of climate model outputs: A generalization of quantile mapping
731 approaches. *Environmetrics* 28(6). <https://doi.org/10.1002/env.2454>
- 732 Déqué M (2007) Frequency of precipitation and temperature extremes over
733 France in an anthropogenic scenario: Model results and statistical correction
734 according to observed values. *Global Planet Change* 57:16 – 26
- 735 Eyring V, Bony S, Meehl GA, et al (2016) Overview of the coupled model inter-
736 comparison project phase 6 (cmip6) experimental design and organization.
737 *Geoscientific Model Development* 9(5):1937–1958. [https://doi.org/10.5194/
738 gmd-9-1937-2016](https://doi.org/10.5194/gmd-9-1937-2016), URL <https://gmd.copernicus.org/articles/9/1937/2016/>
- 739 Faranda D, Vrac M, Yiou P, et al (2020) Changes in future
740 synoptic circulation patterns: Consequences for extreme event
741 attribution. *Geophysical Research Letters* 47(15):e2020GL088,002.
742 <https://doi.org/https://doi.org/10.1029/2020GL088002>, URL [https://
743 //agupubs.onlinelibrary.wiley.com/doi/abs/10.1029/2020GL088002](https://agupubs.onlinelibrary.wiley.com/doi/abs/10.1029/2020GL088002),
744 e2020GL088002 10.1029/2020GL088002, [https://arxiv.org/abs/https://
745 //agupubs.onlinelibrary.wiley.com/doi/pdf/10.1029/2020GL088002](https://arxiv.org/abs/https://agupubs.onlinelibrary.wiley.com/doi/pdf/10.1029/2020GL088002)
- 746 Fisher RA (1915) Frequency distribution of the values of the correlation
747 coefficient in samples from an indefinitely large population. *Biometrika*
748 10(4):507–521. <https://doi.org/10.2307/2331838>
- 749 François B, Vrac M, Cannon AJ, et al (2020) Multivariate bias corrections of
750 climate simulations: which benefits for which losses? *Earth System Dynamics*
751 11(2):537–562. <https://doi.org/10.5194/esd-11-537-2020>, URL [https://esd.
752 copernicus.org/articles/11/537/2020/](https://esd.copernicus.org/articles/11/537/2020/)

- 753 François B, Thao S, Vrac M (2021) Adjusting spatial dependence of climate
754 model outputs with cycle-consistent adversarial networks. *Clim Dyn* <https://doi.org/10.1007/s00382-021-05869-8>
755
- 756 Haddad Z, Rosenfeld D (1997) Optimality of empirical z-r relations. *Q J R*
757 *Meteorol Soc* 123:1283–1293
- 758 Hartigan JA, Wong MA (1979) Algorithm as 136: A k-means clustering algo-
759 rithm. *Journal of the Royal Statistical Society Series C (Applied Statistics)*
760 28(1):100–108. URL <http://www.jstor.org/stable/2346830>
- 761 Hempel S, Frieler K, Warszawski L, et al (2013) A trend-preserving bias
762 correction – the isi-mip approach. *Earth System Dynamics* 4(2):219–236.
763 <https://doi.org/10.5194/esd-4-219-2013>, URL [https://esd.copernicus.org/](https://esd.copernicus.org/articles/4/219/2013/)
764 [articles/4/219/2013/](https://esd.copernicus.org/articles/4/219/2013/)
- 765 Hersbach H, Bell B, Berrisford P, et al (2020) The era5 global
766 reanalysis. *Quarterly Journal of the Royal Meteorological Society*
767 146(730):1999–2049. <https://doi.org/https://doi.org/10.1002/qj.3803>,
768 URL <https://rmets.onlinelibrary.wiley.com/doi/abs/10.1002/qj.3803>,
769 [https://arxiv.org/abs/https://rmets.onlinelibrary.wiley.com/doi/pdf/10.](https://arxiv.org/abs/https://rmets.onlinelibrary.wiley.com/doi/pdf/10.1002/qj.3803)
770 [1002/qj.3803](https://arxiv.org/abs/https://rmets.onlinelibrary.wiley.com/doi/pdf/10.1002/qj.3803)
- 771 Hotelling H (1953) New light on the correlation coefficient and its transforms.
772 *Journal of the Royal Statistical Society Series B (Methodological)* 15(2):193–
773 232. URL <www.jstor.org/stable/2983768>
- 774 Ines AV, Hansen JW (2006) Bias correction of daily gcm rainfall for
775 crop simulation studies. *Agricultural and Forest Meteorology* 138(1):44–
776 53. <https://doi.org/https://doi.org/10.1016/j.agrformet.2006.03.009>, URL
777 <https://www.sciencedirect.com/science/article/pii/S0168192306000979>
- 778 Jézéquel A, Bevacqua E, d’Andrea F, et al (2020) Conditional and resid-
779 ual trends of singular hot days in europe. *Environmental Research Letters*
780 15(6):064,018. <https://doi.org/10.1088/1748-9326/ab76dd>, URL [https://](https://doi.org/10.1088/1748-9326/ab76dd)
781 doi.org/10.1088/1748-9326/ab76dd
- 782 Kallache M, Vrac M, Naveau P, et al (2011) Non-stationary probabilistic
783 downscaling of extreme precipitation. *Journal of Geophysical Research -*
784 *Atmosphere* 116(D05113). <https://doi.org/10.1029/2010JD014892>
- 785 Kay JE, Deser C, Phillips A, et al (2015) The community earth system
786 model (cesm) large ensemble project: A community resource for study-
787 ing climate change in the presence of internal climate variability. *Bul-*
788 *letin of the American Meteorological Society* 96(8):1333 – 1349. [https://](https://doi.org/10.1175/BAMS-D-13-00255.1)
789 doi.org/10.1175/BAMS-D-13-00255.1, URL [https://journals.ametsoc.org/](https://journals.ametsoc.org/view/journals/bams/96/8/bams-d-13-00255.1.xml)
790 [view/journals/bams/96/8/bams-d-13-00255.1.xml](https://journals/bams/96/8/bams-d-13-00255.1.xml)

- 791 Kendon EJ, Rowell DP, Jones RG, et al (2008) Robustness of future changes in
792 local precipitation extremes. *Journal of Climate* 21(17):4280 – 4297. <https://doi.org/10.1175/2008JCLI2082.1>, URL <https://journals.ametsoc.org/view/journals/clim/21/17/2008jcli2082.1.xml>
- 795 Laux P, Rötter RP, Webber H, et al (2021) To bias correct or not to bias
796 correct? an agricultural impact modelers’ perspective on regional climate
797 model data. *Agricultural and Forest Meteorology* 304-305:108,406. <https://doi.org/https://doi.org/10.1016/j.agrformet.2021.108406>, URL <https://www.sciencedirect.com/science/article/pii/S0168192321000897>
- 800 Maraun D, Truhetz H, Schaffer A (2021) Regional climate model
801 biases, their dependence on synoptic circulation biases and the
802 potential for bias adjustment: A process-oriented evaluation of
803 the austrian regional climate projections. *Journal of Geophysical
804 Research: Atmospheres* 126(6):e2020JD032,824. <https://doi.org/https://doi.org/10.1029/2020JD032824>, URL <https://agupubs.onlinelibrary.wiley.com/doi/abs/10.1029/2020JD032824>,
805 <https://arxiv.org/abs/https://agupubs.onlinelibrary.wiley.com/doi/pdf/10.1029/2020JD032824>,
806 <https://arxiv.org/abs/https://agupubs.onlinelibrary.wiley.com/doi/pdf/10.1029/2020JD032824>,
807 <https://arxiv.org/abs/https://agupubs.onlinelibrary.wiley.com/doi/pdf/10.1029/2020JD032824>
808
- 809 Matte D, Larsen MAD, Christensen OB, et al (2019) Robustness and
810 scalability of regional climate projections over europe. *Frontiers in Envi-
811 ronmental Science* 6:163. <https://doi.org/10.3389/fenvs.2018.00163>, URL
812 <https://www.frontiersin.org/article/10.3389/fenvs.2018.00163>
- 813 Mengis N, Keller D, Rickels W, et al (2019) Climate engineering–induced
814 changes in correlations between earth system variables—implications
815 for appropriate indicator selection. *Climatic Change* 153:305–322.
816 <https://doi.org/10.1007/s10584-019-02389-7>, URL <https://doi.org/10.1007/s10584-019-02389-7>
817
- 818 Michelangeli PA, Vautard R, Legras B (1995) Weather regimes:
819 Recurrence and quasi stationarity. *Journal of Atmospheric Sciences*
820 52(8):1237 – 1256. [https://doi.org/10.1175/1520-0469\(1995\)052\(1237:
821 WRRAQ5\)2.0.CO;2](https://doi.org/10.1175/1520-0469(1995)052(1237:WRRAQ5)2.0.CO;2), URL [https://journals.ametsoc.org/view/journals/
822 atsc/52/8/1520-0469_1995_052_1237_wrraqs_2_0_co_2.xml](https://journals.ametsoc.org/view/journals/atsc/52/8/1520-0469_1995_052_1237_wrraqs_2_0_co_2.xml)
- 823 Piani C, Haerter JO (2012) Two dimensional bias correction of temperature
824 and precipitation copulas in climate models. *Geophys Res Lett* <https://doi.org/10.1029/2012GL053839>
- 826 Riahi K, van Vuuren DP, Kriegler E, et al (2017) The shared socioeco-
827 nomic pathways and their energy, land use, and greenhouse gas emis-
828 sions implications: An overview. *Global Environmental Change* 42:153–
829 168. <https://doi.org/https://doi.org/10.1016/j.gloenvcha.2016.05.009>, URL
830 <https://www.sciencedirect.com/science/article/pii/S0959378016300681>

- 831 Ridder NN, Pitman AJ, Ukkola AM (2021) Do cmip6 climate mod-
832 els simulate global or regional compound events skillfully? *Geophysical*
833 *Research Letters* 48(2):e2020GL091152. [https://doi.org/https://doi.org/](https://doi.org/https://doi.org/10.1029/2020GL091152)
834 [10.1029/2020GL091152](https://doi.org/https://doi.org/10.1029/2020GL091152)
- 835 Robin Y, Vrac M (2021) Is time a variable like the others in multivariate
836 statistical downscaling and bias correction? *Earth System Dynamics Dis-*
837 *cussions* 2021:1–32. <https://doi.org/10.5194/esd-2021-12>, URL [https://esd.](https://esd.copernicus.org/preprints/esd-2021-12/)
838 [copernicus.org/preprints/esd-2021-12/](https://esd.copernicus.org/preprints/esd-2021-12/)
- 839 Robin Y, Vrac M, Naveau P, et al (2019) Multivariate stochastic bias cor-
840 rections with optimal transport. *Hydrol Earth Syst Sci* 23:773–786. <https://doi.org/10.5194/hess-23-773-2019>
- 842 Rust HW, Vrac M, Sultan B, et al (2013) Mapping weather-type
843 influence on senegal precipitation based on a spatial–temporal sta-
844 tistical model. *Journal of Climate* 26(20):8189 – 8209. [https://doi.](https://doi.org/10.1175/JCLI-D-12-00302.1)
845 [org/10.1175/JCLI-D-12-00302.1](https://doi.org/10.1175/JCLI-D-12-00302.1), URL [https://journals.ametsoc.org/view/](https://journals.ametsoc.org/view/journals/clim/26/20/jcli-d-12-00302.1.xml)
846 journals/clim/26/20/jcli-d-12-00302.1.xml
- 847 Sadegh M, Moftakhari H, Gupta HV, et al (2018) Multihazard scenarios
848 for analysis of compound extreme events. *Geophysical Research Letters*
849 45(11):5470–5480. <https://doi.org/https://doi.org/10.1029/2018GL077317>
- 850 Seferian R (2018) CNRM-CERFACS CNRM-ESM2-1 model output pre-
851 pared for CMIP6 CMIP. <https://doi.org/10.22033/ESGF/CMIP6.1391>,
852 URL <https://doi.org/10.22033/ESGF/CMIP6.1391>
- 853 Seo S, Das Bhowmik R, Sankarasubramanian A, et al (2019) The role
854 of cross-correlation between precipitation and temperature in basin-scale
855 simulations of hydrologic variables. *Journal of Hydrology* 570:304–314.
856 <https://doi.org/https://doi.org/10.1016/j.jhydrol.2018.12.076>, URL [https://](https://www.sciencedirect.com/science/article/pii/S002216941930054X)
857 www.sciencedirect.com/science/article/pii/S002216941930054X
- 858 Shiogama H, Abe M, Tatebe H (2019) MIROC MIROC6 model output pre-
859 pared for CMIP6 ScenarioMIP. [https://doi.org/10.22033/ESGF/CMIP6.](https://doi.org/10.22033/ESGF/CMIP6.898)
860 [898](https://doi.org/10.22033/ESGF/CMIP6.898), URL <https://doi.org/10.22033/ESGF/CMIP6.898>
- 861 Singh H, Najafi M, Cannon A (2021) Characterizing non-stationary com-
862 pound extreme events in a changing climate based on large-ensemble
863 climate simulations. *Clim Dyn* 56:1389—1405. [https://doi.org/10.1007/](https://doi.org/10.1007/s00382-020-05538-2)
864 [s00382-020-05538-2](https://doi.org/10.1007/s00382-020-05538-2)
- 865 Sukharev J, Wang C, Ma KL, et al (2009) Correlation study of time-varying
866 multivariate climate data sets. In: 2009 IEEE Pacific Visualization Symposi-
867 um, pp 161–168, <https://doi.org/10.1109/PACIFICVIS.2009.4906852>

- 868 Swart NC, Cole JN, Kharin VV, et al (2019) CCCma CanESM5 model out-
869 put prepared for CMIP6 ScenarioMIP. [https://doi.org/10.22033/ESGF/](https://doi.org/10.22033/ESGF/CMIP6.1317)
870 [CMIP6.1317](https://doi.org/10.22033/ESGF/CMIP6.1317), URL <https://doi.org/10.22033/ESGF/CMIP6.1317>
- 871 Tang Y, Rumbold S, Ellis R, et al (2019) MOHC UKESM1.0-LL model out-
872 put prepared for CMIP6 CMIP historical. [https://doi.org/10.22033/ESGF/](https://doi.org/10.22033/ESGF/CMIP6.6113)
873 [CMIP6.6113](https://doi.org/10.22033/ESGF/CMIP6.6113), URL <https://doi.org/10.22033/ESGF/CMIP6.6113>
- 874 Teutschbein C, Seibert J (2012) Bias correction of regional climate model
875 simulations for hydrological climate-change impact studies: Review and eval-
876 uation of different methods. *Journal of Hydrology* 456-457:12–29. [https://](https://doi.org/https://doi.org/10.1016/j.jhydrol.2012.05.052)
877 doi.org/https://doi.org/10.1016/j.jhydrol.2012.05.052, URL [https://www.](https://www.sciencedirect.com/science/article/pii/S0022169412004556)
878 [sciencedirect.com/science/article/pii/S0022169412004556](https://www.sciencedirect.com/science/article/pii/S0022169412004556)
- 879 Tukimat NNA, Harun S, Tadza MYM (2019) The potential of canoni-
880 cal correlation analysis in multivariable screening of climate model. *IOP*
881 *Conference Series: Earth and Environmental Science* 365:012,025. [https://](https://doi.org/10.1088/1755-1315/365/1/012025)
882 doi.org/10.1088/1755-1315/365/1/012025, URL [https://doi.org/10.1088/](https://doi.org/10.1088/1755-1315/365/1/012025)
883 [1755-1315/365/1/012025](https://doi.org/10.1088/1755-1315/365/1/012025)
- 884 Voldoire A (2018) CNRM-CERFACS CNRM-CM6-1 model output pre-
885 pared for CMIP6 CMIP. <https://doi.org/10.22033/ESGF/CMIP6.1375>,
886 URL <https://doi.org/10.22033/ESGF/CMIP6.1375>
- 887 Voldoire A (2019) CNRM-CERFACS CNRM-CM6-1-HR model output pre-
888 pared for CMIP6 HighResMIP. [https://doi.org/10.22033/ESGF/CMIP6.](https://doi.org/10.22033/ESGF/CMIP6.1387)
889 [1387](https://doi.org/10.22033/ESGF/CMIP6.1387), URL <https://doi.org/10.22033/ESGF/CMIP6.1387>
- 890 Volodin E, Mortikov E, Gritsun A, et al (2019) INM INM-CM5-0 model out-
891 put prepared for CMIP6 CMIP abrupt-4xCO2. [https://doi.org/10.22033/](https://doi.org/10.22033/ESGF/CMIP6.4932)
892 [ESGF/CMIP6.4932](https://doi.org/10.22033/ESGF/CMIP6.4932), URL <https://doi.org/10.22033/ESGF/CMIP6.4932>
- 893 Volosciuk C, Maraun D, Vrac MM. andWidmann (2017) A combined statistical
894 bias correction and stochastic downscaling method for precipitation. *Hydrol*
895 *Earth Syst Sci* 21:1693–1719. <https://doi.org/10.5194/hess-21-1693-2017>
- 896 Vrac M (2018) Multivariate bias adjustment of high-dimensional climate sim-
897 ulations: the rank resampling for distributions and dependences (r2d2)
898 bias correction. *Hydrology and Earth System Sciences* 22:3175–3196. [https://](https://doi.org/https://doi.org/10.5194/hess-22-3175-2018)
899 doi.org/https://doi.org/10.5194/hess-22-3175-2018
- 900 Vrac M, Drobinski P, Merlo A, et al (2012) Dynamical and statistical down-
901 scaling of the French Mediterranean climate: uncertainty assessment. *Nat*
902 *Hazards Earth Syst Sci* 12:2769–2784, doi:10.5194/nhess-12-2769-2012

- 903 Vrac M, Noël T, Vautard R (2016) Bias correction of precipitation
904 through Singularity Stochastic Removal: Because occurrences matter. *Journal of Geophysical Research: Atmospheres* 121. [https://doi.org/10.1002/](https://doi.org/10.1002/2015JD024511)
905 [2015JD024511](https://doi.org/10.1002/2015JD024511)
906
- 907 Wu T, Chu M, Dong M, et al (2018) BCC BCC-CSM2MR model out-
908 put prepared for CMIP6 CMIP piControl. [https://doi.org/10.22033/ESGF/](https://doi.org/10.22033/ESGF/CMIP6.3016)
909 [CMIP6.3016](https://doi.org/10.22033/ESGF/CMIP6.3016), URL <https://doi.org/10.22033/ESGF/CMIP6.3016>
- 910 You P, Nogaj M (2004) Extreme climatic events and weather regimes
911 over the north atlantic: When and where? *Geophysical Research Let-*
912 *ters* 31(7). <https://doi.org/https://doi.org/10.1029/2003GL019119>, URL
913 <https://agupubs.onlinelibrary.wiley.com/doi/abs/10.1029/2003GL019119>,
914 [https://arxiv.org/abs/https://agupubs.onlinelibrary.wiley.com/doi/pdf/10.](https://arxiv.org/abs/https://agupubs.onlinelibrary.wiley.com/doi/pdf/10.1029/2003GL019119)
915 [1029/2003GL019119](https://arxiv.org/abs/https://agupubs.onlinelibrary.wiley.com/doi/pdf/10.1029/2003GL019119)
- 916 You P, Cattiaux J, Ribes A, et al (2018) Recent trends in the recurrence of
917 north atlantic atmospheric circulation patterns. *Complexity* 2018(Article ID
918 3140915). <https://doi.org/10.1155/2018/3140915>
- 919 Yukimoto S, Koshiro T, Kawai H, et al (2019) MRI MRI-ESM2.0 model output
920 prepared for CMIP6 CMIP. <https://doi.org/10.22033/ESGF/CMIP6.621>,
921 URL <https://doi.org/10.22033/ESGF/CMIP6.621>
- 922 Zscheischler J, Seneviratne SI (2017) Dependence of drivers affects risks asso-
923 ciated with compound events. *Science Advances* 3(6). [https://doi.org/10.](https://doi.org/10.1126/sciadv.1700263)
924 [1126/sciadv.1700263](https://doi.org/10.1126/sciadv.1700263), URL [https://advances.sciencemag.org/content/3/6/](https://advances.sciencemag.org/content/3/6/e1700263)
925 [e1700263](https://advances.sciencemag.org/content/3/6/e1700263), [https://arxiv.org/abs/https://advances.sciencemag.org/content/](https://arxiv.org/abs/https://advances.sciencemag.org/content/3/6/e1700263.full.pdf)
926 [3/6/e1700263.full.pdf](https://arxiv.org/abs/https://advances.sciencemag.org/content/3/6/e1700263.full.pdf)
- 927 Zscheischler J, Fischer EM, Lange S (2019) The effect of univariate bias adjust-
928 ment on multivariate hazard estimates. *Earth System Dynamics* 10(1):31–
929 43. <https://doi.org/10.5194/esd-10-31-2019>, URL [https://esd.copernicus.](https://esd.copernicus.org/articles/10/31/2019/)
930 [org/articles/10/31/2019/](https://esd.copernicus.org/articles/10/31/2019/)
- 931 Zscheischler J, Martius O, Westra S, et al (2020) A typology of compound
932 weather and climate events. *Nat Rev Earth Environ* 1:333–347. <https://doi.org/10.1038/s43017-020-0060-z>
933
- 934 Zscheischler J, Naveau P, Martius O, et al (2021) Evaluating the dependence
935 structure of compound precipitation and wind speed extremes. *Earth System*
936 *Dynamics* 12(1):1–16. <https://doi.org/10.5194/esd-12-1-2021>, URL [https://](https://esd.copernicus.org/articles/12/1/2021/)
937 esd.copernicus.org/articles/12/1/2021/

Simulation name	Run	Atmospheric resolution	Data reference
BCC-CSM2-MR	r1i1p1f1	100 km	Wu et al (2018)
CanESM5	r10i1p1f1	500 km	Swart et al (2019)
CNRM-CM6-1-HR	r1i1p1f2	100 km	Voltaire (2019)
CNRM-CM6-1	r1i1p1f2	250 km	Voltaire (2018)
CNRM-ESM2-1	r1i1p1f2	250 km	Seferian (2018)
INM-CM4-8	r1i1p1f1	100 km	Volodin et al (2019)
INM-CM5-0	r1i1p1f1	100 km	Volodin et al (2019)
IPSL-CM6A-LR	r14i1p1f1	250 km	Boucher et al (2018)
MIROC6	r1i1p1f1	250 km	Shiogama et al (2019)
MRI-ESM2-0	r1i1p1f1	100 km	Yukimoto et al (2019)
UKESM1-0-LL	r1i1p1f2	250 km	Tang et al (2019)

Table 1 List of CMIP6 simulations used in this study, their run, approximate horizontal resolution and references.

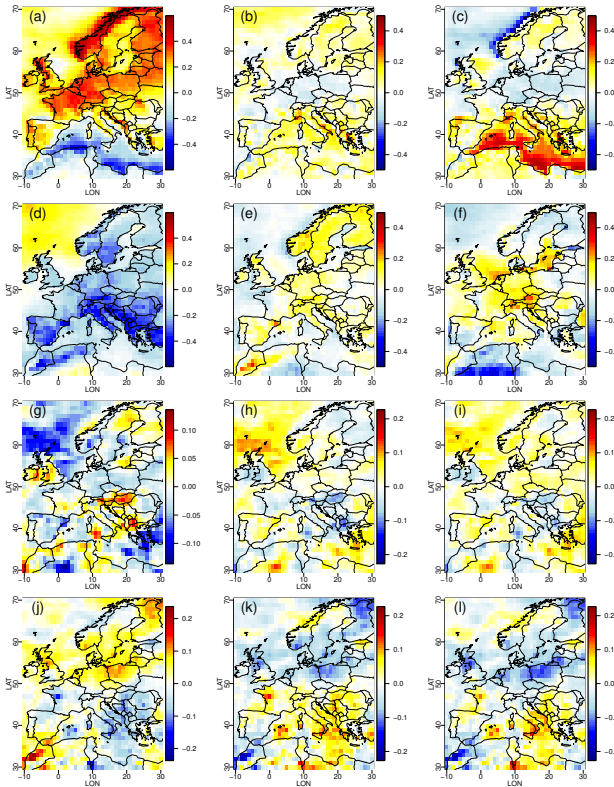


Fig. 1 First two rows: (a, d) Maps of 1980-1999 ERA5 inter-variable (temperature, precipitation) correlations; (b, e) Biases of CMIP6 inter-variable correlations with respect to ERA5 correlations; (c, e) Biases of CISM inter-variable correlations with respect to ERA5 correlations. Last two rows: (g, j) Maps of changes (from 1980-1999 to 2000-2019) in ERA5 inter-variable (temperature, precipitation) correlations; (h, k) Biases of CMIP6 in changes of inter-variable correlations; (i, l) Biases of CISM in changes of inter-variable correlations. First row (a, b, c) and third one (g, h, i) correspond to winter results, while second (d, e, f) and fourth (j, k, l) ones correspond to summer results. The equivalent maps for spring and fall are provided as supplementary materials in Figure [SM.1](#).

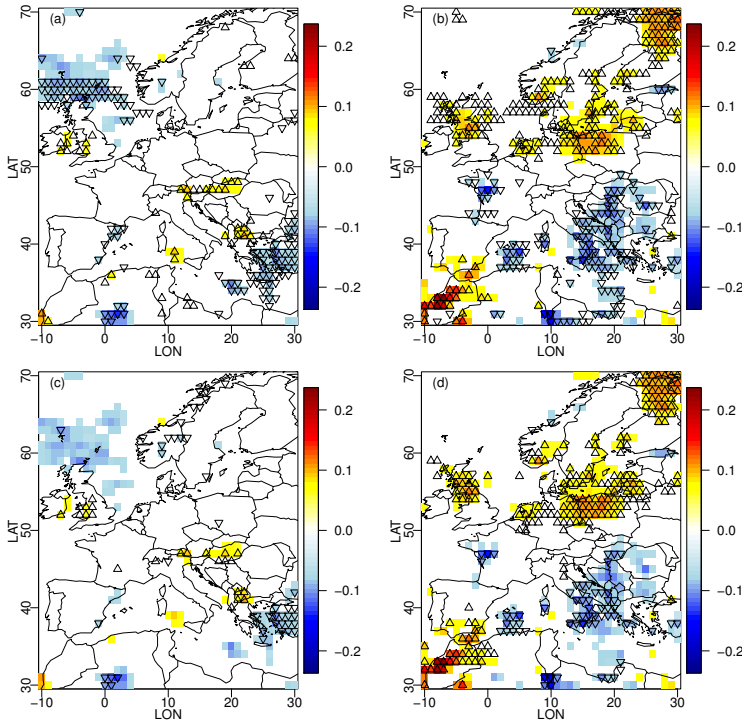


Fig. 2 Colours: significant changes in ERA5 (temperature vs. precipitation) Pearson correlations from 1980-1999 to 2000-2019. Symbols: upper triangles show where the ERA5 change in correlation is higher than the 95th percentile from the ensemble of correlation changes; lower triangles correspond to ERA5 change in correlation lower than the 5th percentile. Results are shown for CMIP6 (a, b) and CESM (c, d), for winter (a, c) and summer (b, d). Results for spring and fall are given in Figure SM.2 of the supplementary materials.

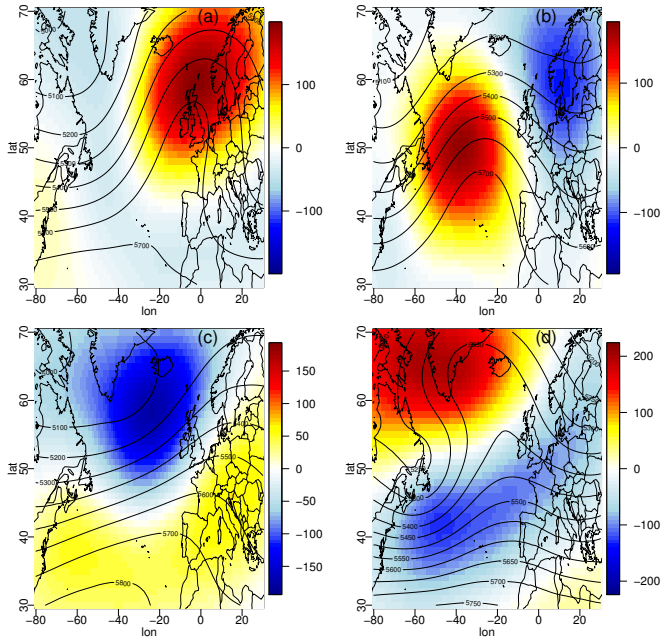


Fig. 3 Composite maps of the four ERA5 winter clusters obtained from the k-means algorithm applied to daily fields of z500 over the north Atlantic region. Colours correspond to z500 anomalies and contours to raw z500. The equivalent composite maps for the other seasons are given as supplementary materials in Figures SM.3 to SM.5.

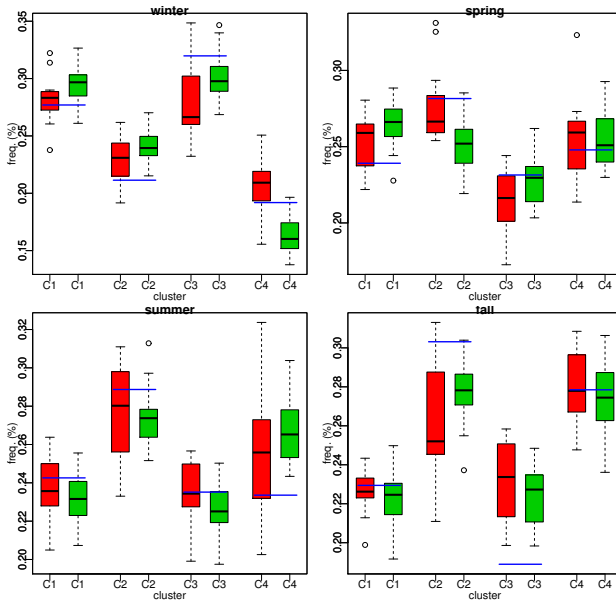


Fig. 4 For each season, boxplots of frequencies of z500 regimes occurrences for CMIP6 (in red) and CESM simulations (in green). The blue segments correspond to the ERA5 frequencies of the regimes.

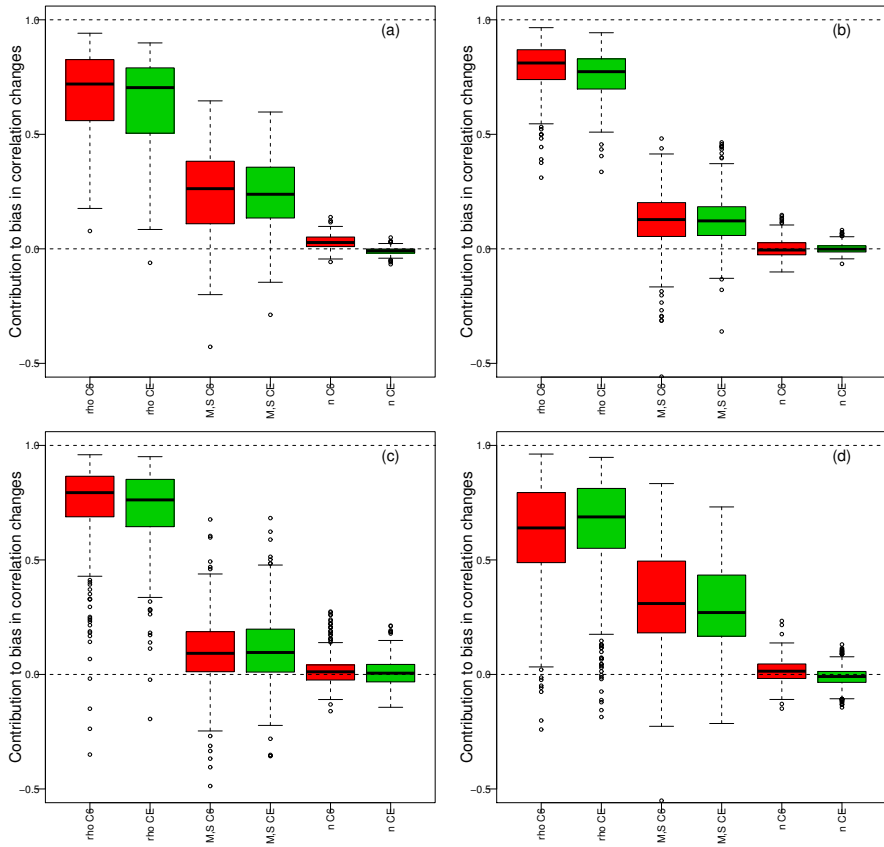


Fig. 5 Boxplots of mean influence values of the three **WRCI** components to the biases in changes of temperature-precipitation correlations from 1980-1999 to 2000-2019 in (a) winter, (b) spring, (c) summer, (d) fall. All CMIP6 (red) and CESM (green) boxplots show the spatial variability of the influence results averaged by ensemble for each gridcell. The associated maps are provided as supplementary materials in Figures [SM.14](#) to [SM.17](#).

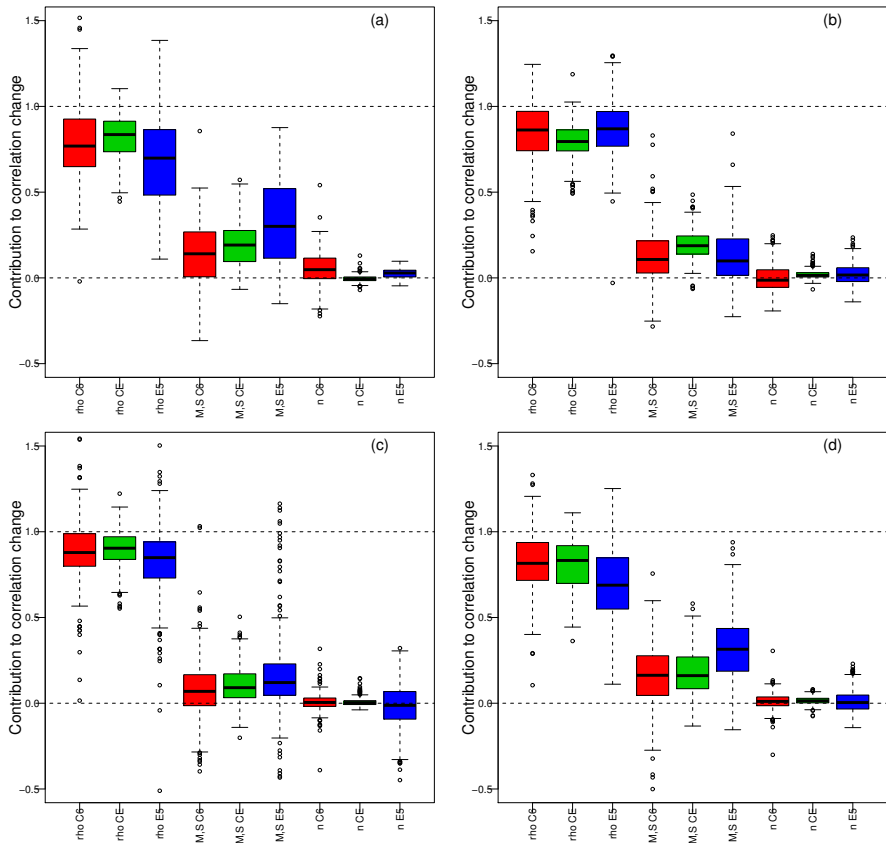


Fig. 6 Boxplots of contribution values of the changes in the three **WRCI** components to the changes in temperature-precipitation correlations from 1980-1999 to 2000-2019 in (a) winter, (b) spring, (c) summer, (d) fall. All CMIP6 (red), CESM (green) and ERA5 (blue) boxplots show the spatial variability of the results. The associated maps are provided as supplementary materials in Figures [SM.18](#) – [SM.21](#).

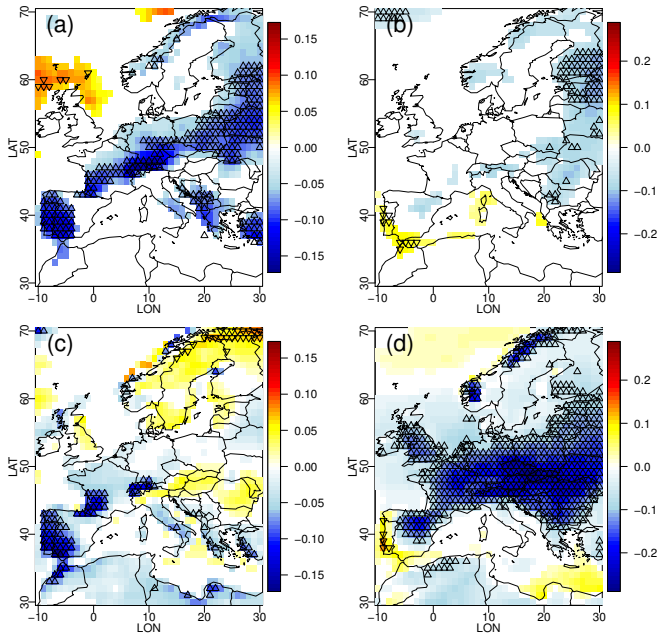


Fig. 7 Colours: Significant mean differences in correlations from 1981-2000 to 2081-2100; Symbols: upper triangles show where $\pi_0 > 0.95$; lower triangles correspond to $\pi_0 < 0.05$. Results are shown for CMIP6 (a, b) and CESM (c,d), for winter (a, c) and summer (b, d). The equivalent maps for spring and fall are given as supplementary materials in Fig. SM.22.

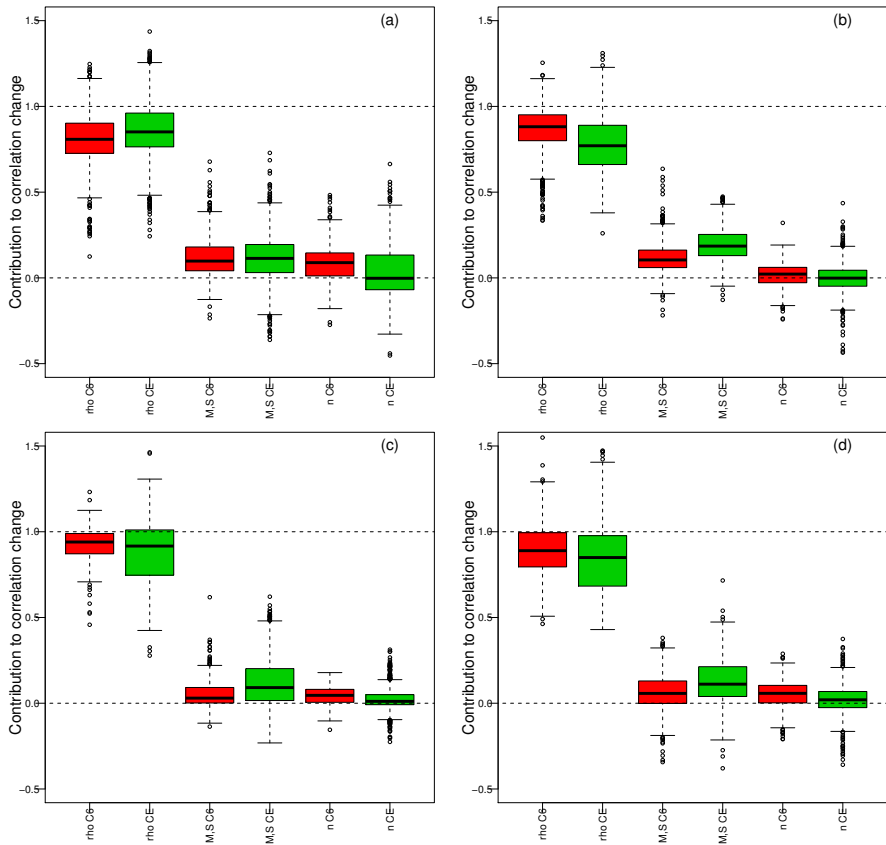


Fig. 8 Same as Fig. 6 but for future changes: Boxplots of contributions of change of the three WRCIs to the changes in temperature-precipitation correlations from 1981-2000 to 2081-2100 in (a) winter, (b) spring, (c) summer, (d) fall. Red boxplots are for CMIP6 and green ones for CESM. All boxplots show the spatial variability of the results.

Supplementary Files

This is a list of supplementary files associated with this preprint. Click to download.

- [SuppVracetal2021ClimDynChangesincorr.pdf](#)